Vol. 42, No. 3 (2020) 503-512, DOI: 10.24874/ti.964.09.20.09

Tribology in Industry

www.tribology.rs

RESEARCH

Experimental Study and Analytical model of Shear Thinning in 3D Bioprinting of Gelatin

N. Busarac[a], Ž. Jovanović[a], S. Njezić[b], F. Živić[a,*], N. Grujović[a], D. Adamović[a]

[a]*Faculty of Engineering, University of Kragujevac, Sestre Janjić 6, Kragujevac, Serbia,*
[b]*Faculty of Medicine, University of Banja Luka, Save Mrkalja 14, Banja Luka, Bosnia and Herzegovina.*

Keywords:

Gelatin
3D Bioprinting
Shear thinning
Friction factor
Bioinks

* Corresponding author:

Fatima Živić
E-mail: zivic@kg.ac.rs

Received: 13 June 2020
Revised: 24 July 2020
Accepted: 26 August 2020

A B S T R A C T

This paper presented extrusion-based 3D bioprinting of gelatin hydrogel and optimisation of material properties and process parameters, in order to improve printability of hydrogel. Gelatin hydrogel was prepared by mixing it with water in concentration of 13.04 wt%. Dimensional accuracy of the bioprinting was studied and significant changes in comparison with designed geometry were noted. Gelatin hydrogel made only with water showed inadequate thixotropy for extrusion based bioprinting and poor mechanical properties of the printed sample, and needs additional constituents to enable good printability with satisfying dimensional accuracy. We presented parameter optimisation index (POI), shear thinning model and friction factor of gelatin hydrogel by using analytical approach. Friction factor of the gelatin hydrogel during bioprinting was $0.268 \cdot 10^{-5}$. Analytical models of shear thinning and friction factor were in consistence with experimental data, and indicated that such approach can be used in optimisation of bioprinting parameters and material properties.

1. INTRODUCTION

Additive manufacturing (AM) represents production technologies in which the product is fabricated by successively adding layers of material upon each other. They have found application in various fields. 3D bioprinting is emerging as one of the AM technologies with application in bioengineering for fabrication of scaffolds that can be used for cell seeding or even organ printing [1]. Three dimensional (3D) bioprinting is state-of-the-art research area by involving combination of cells, growth factors, and biomaterials to fabricate biomedical parts that maximally mimic natural tissue characteristics [2]. Range of materials is under research for the use in bioprinting. Materials that have been used for 3D bioprinting (often called bioinks) are natural polymers, such as collagen [3], gelatin [4], alginate [5], hyaluronic acid (HA) [6], and synthetic polymers, such as PVA [7] and polyethylene glycol (PEG).

Gelatin is one of the basic materials that is studied for use in bioprinting, but it usually needs some additives or chemical crosslinking to achieve good printability and mechanical properties of bioscaffold. There are many

material combinations that have been experimentally tried to improve gelatin-based hydrogels, such as crosslinking with microbial transglutaminase (mTgase), in order to print cell bearing hydrogels [8]. However, exactly determined material and process parameters for gelatin-based hydrogels in bioprinting are still under research. Bioprinting technologies are also under research, whereas extrusion-based bioprinting has been the most studied since it is low cost and efficient technology.

Rheological behaviour of hydrogels is of the utmost importance in bioprinting. For extrusion-based bioprinting, one of the main influential factors on material behaviour is shear thinning property that is closely related to material printability and dimensional accuracy [9]. Shear strain during bioprinting was not experimentally measured, since soft materials in bioprinting tend to behave differently than standard hard engineering materials, for which there are experimental measurement techniques. Analytical solutions for shear thinning involve complex continuum and fluid mechanics and are also under research. Modeling of bioprinting must consider complex physical and chemical phenomenon during the process [10], and shear thinning and fluid dynamic of the hydrogel is of the utmost importance for understanding the process.

In this paper, we experimentally tested extrusion-based 3D bioprinting of gelatin mixed with water and determined the most influential factors on the quality of printed sample. We presented analytical solution for shear thinning and friction factor and validated it by using data from bioprinting experiment. We introduced parameter optimization index (POI) in extrusion-based 3D bioprinting. There is a need for further study, but this investigation showed that combination of experimental trials, and optimisation methods with theoretical physics and fluid mechanics can efficiently assist in getting the optimal set of printing parameters, and material properties, aiming at design and fabrication of bioscaffolds.

2. 3D BIOPRINTING TECHNOLOGIES

Extrusion-based bioprinting is the most used method of 3D bioprinting, where complex 3D structures are created by extruding the material in a form of filament. The main requirement of the extrusion-based bioprinting is prevention of droplet formation. Instead, thin filament-like soft material is forming 3D scaffolds. Droplet-based 3D bioprinting, utilizes the formation of discrete droplets, by using some of the methods such as electrohydrodynamic jetting, inkjet bioprinting and laser-assisted bioprinting. Three most common methods of 3D bioprinting are shown in Fig. 1.

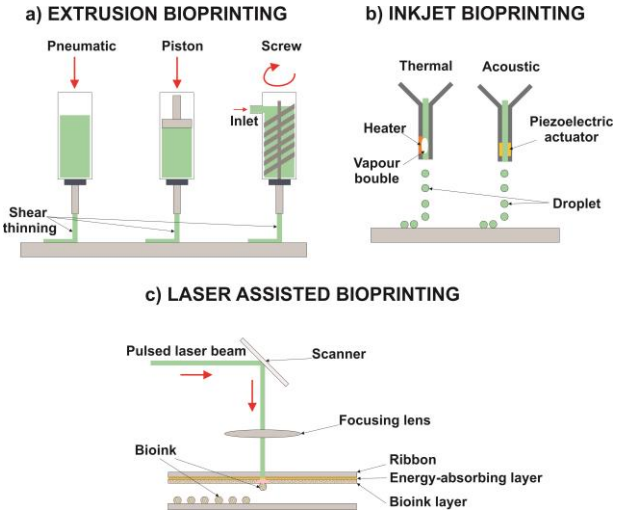

Fig. 1. Three most common methods of 3D bioprinting.

Extrusion-based bioprinting is suitable for soft materials that exhibit shear thinning property. Shear thinning is usually associated with non-Newtonian fluids (or in this case hydrogels), where its viscosity decreases under shear strain. Accordingly, such hydrogels subjected to pressure during extrusion form thin filament at the output of the syringe, instead of the droplet. However, not all materials have shear thinning property and cannot be used in extrusion bioprinting. Droplet-based bioprinting has higher accuracy but the availability of 3D printers is scarce. In general, this is very interesting research area from aspect of biomedical applications. Laser-assisted bioprinting has higher resolution than inkjet method and solves the clogging problem because it is not using the nozzle, but it is still at the very beginning of research. Development of 3D bioprinting is conditioned by the development of bioinks, or suitable materials for bioprinting. Different composite hydrogels are studied aiming at optimal material properties for extrusion-based bioprinting, as simple and low cost solution.

High accuracy of details is necessary in order to mimic the structures of native tissue. Often, this imposes limitation on extrusion-based method. Using nozzle tips or needles with a smaller diameter should provide higher accuracy but clogging problems often arise when combining small diameters and viscous materials. Another issue can be decrease in cell viability due to higher shear stress. Materials with higher viscosity have favourable mechanical properties and retain shape easier than hydrogels with lower viscosity. Perfect material for extrusion-based bioprinting would have a viscosity high enough to retain shape of a complex multi-layer 3D structure, and exhibit shear thinning during the process of extrusion through the nozzle. It should become thinner during extrusion, restore its original thickness afterwards, within 3D structure and also, exhibit some degree of hardening after extrusion, in controlled manner. This is yet very difficult to achieve. If hydrogel does not have these properties, it is usually cross-linked with some suitable agents, or further mixed to form composite structure. Using secondary-crosslinking when printing with lower viscosity hydrogel can be a successful approach also to ensure cell viability. Beside viscosity, surface tension has governing influence on either filament or droplet formation during extrusion, whereas low surface tension is favourable [11].

2.1 Gelatin and gelatin-based hydrogels

One of the most common materials for soft biocompatible scaffolds, and widely used in biomedical research, is gelatin. Gelatin is polypeptide mixture derived from collagen through the process of partial hydrolysis. It is biocompatible and promotes adhesion, migration, proliferation and differentiation of cells. However, gelatin forms thermo-reversible hydrogel which is not stable. Chemical modifications and crosslinking are usually used to overcome this issue. Its properties, in general, depend on the origin. Gelatin derived from collagen taken from animal body parts has humanlike polypeptides, and gelatin derived from fish has lower melting and gel points and higher viscosity. Average molecule length and molecular weight of gelatin polypeptide depends on the origin of the material and the process of hydrolysis.

Gelatin-based hydrogels are made by cooling a gelatin solution, basically with water. Gelatin is water-soluble and can absorb up to 10 times its weight in water. Temperature, pH, concentration and method of preparation all significantly influence the behavior of gelatin solution or resulting hydrogel. Typically, gelation (gel transition) occurs at low temperatures in a range of 20 – 30 °C. Hydrogen bonds, electrostatic and hydrophobic bonds are created during the sol – gel transition, which are thermo-reversible. Such hydrogels are used for 3D bioprinting of scaffolds, aiming to support cell function and proliferation, or to form sacrificial material for further processing of final biomaterials.

One of the main requirements for the scaffold is to exhibit appropriate mechanical properties that are closely linked to the concentration of the hydrogel solution. Other important properties are temperature, pH, viscosity, and presence of additives or other agents. Mechanical strength and rigidity are low because gelatin-based hydrogels are created through physical crosslinking. Since many applications require better mechanical properties, methods of improvement have been studied. Mixing of gelatin with other substances is an easy and effective method. GelMA (gelatin-methacrylamide) is a hybrid hydrogel created by mixing gelatin and methacrylate that has better printability and viscosity compared to gelatin-only hydrogels. Higher mechanical strength and print accuracy can be achieved after photopolymerization of GelMA, using photoinitiators and UV light. Another effective method is chemical crosslinking of polymer chains, to create bigger macromolecules. But some issues are recognised with chemical reagents, such as with aldehyde, that is toxic for cells even when the cells are encapsulated [12].

3. PARAMETER OPTIMIZATION INDEX (POI) IN EXTRUSION-BASED 3D BIOPRINTING

There are many influential variables in the extrusion bioprinting that affect the final quality of the printed scaffold. Experimental studies are conducted to find optimal set of parameters (printing speed, fluid velocity, dimensional properties, etc.), but material properties essentially determine the printability.

Considering numerous mutually dependent process parameters, available methods of parameter optimisation should provide directions to get the best scaffold with necessary properties.

Understanding the relationship between accuracy and shear stress is very important for the bioprinting process. Accuracy A can be measured experimentally by measuring printing line width l (equation 1), while shear stress τ is usually analytically described. Standard experimental methods to determine shear stress are not yet applicable for extrusion of soft materials. The relationship between pressure p, nozzle diameter D and shear stress τ (equation 2) is known in fluid mechanics. According to [13], parameter optimization index (POI) can be introduced to maximize accuracy and minimize shear stress (equation 3) and (equation 4), where needle gauge G refers to the needle opening size, where the bigger gauge means smaller diameter.

$$A \sim \frac{1}{l} \tag{1}$$

$$\frac{1}{\tau} \sim \frac{D}{p} \tag{2}$$

$$POI = A \cdot \frac{1}{\tau} \tag{3}$$

$$POI = \frac{1}{l \cdot G \cdot p} \tag{4}$$

Optimization index (POI) for a specific material across a range of printing parameter can be normalised relative to the maximum POI in series of tests, as shown in (equation 5), where i denotes POI for individual set of parameters; MAX,n denotes the maximum POI of the entire range tested; and n is the number of discrete combinations of tested parameter [13].

$$POI_i = \frac{POI_i}{POI_{MAX,n}} \tag{5}$$

In case of incompressible fluids (such as hydrogel solution in extrusion bioprinting), Bernoulli's equation is valid. Two specific points for the flow of hydrogel during bioprinting can be setup: the first one where syringe plunger touches the solution and the second one at the needle tip. Pressure at the point where hydrogel leaves the needle is atmospheric pressure and height reference plane can be chosen as h_1=0, h_2-h_1=h. Accordingly, the relationship between fluid flow velocity and pressure can be given as in equation 6, where P refers to absolute pressure; ρ is solution density; v is fluid flow velocity at streamline; g is gravitational acceleration; and h refers to height (or hydraulic head). From this equation POI can be calculated with experimental data.

$$p + \frac{1}{2}\rho v_1^2 = \frac{1}{2}\rho v_2^2 + \rho g h \tag{6}$$

3.1 Shear-thinning model and friction factor in extrusion-based 3D bioprinting

Assuming negligible fluid and particle inertia, the fluid dynamics of the investigated system is governed by the following mass and momentum balance equations [10,14-16], as given in equations 7-10, where u - velocity; τ – shear stress tensor; p – pressure; I – unit tensor (3x3); η – viscosity; σ – strain rate tensor, and T means that velocity vector is transposed.

$$\nabla \vec{u} = 0 \tag{7}$$

$$\nabla \vec{\tau} = 0 \tag{8}$$

$$\vec{\tau} = -p\vec{I} + 2\eta(\dot{\gamma})\vec{\sigma} \tag{9}$$

$$\vec{\sigma} = \frac{\nabla \vec{u} + (\nabla \vec{u})^T}{2} \tag{10}$$

Tensor σ is traceless trσ=0 (traceless stress tensor) and pressure is consistent with the continuity equation. The tracefree requirement together with the physical requirement of symmetry $\sigma = \sigma^T$ imply that there are only three independent shear components (off – diagonal elements) and two normal stress differences (diagonal elements) of the deviatoric stress. Thus, in Cartesian coordinates equations 11-13 are valid.

$$\sigma_{xy} = \sigma_{yx} \tag{11}$$

$$\sigma_{xz} = \sigma_{zx} \tag{12}$$

$$\sigma_{yz} = \sigma_{zy} \tag{13}$$

We model the suspending fluid by the power-law constitutive equation 14, where m is the consistency index – (viscosity factor); and n is the flow index and ϒ effective deformation rate or rate of shear. Accordingly, equation 15 is valid.

$$\eta(\dot{\gamma}) = m\dot{\gamma}^{n-1} \tag{14}$$

$$\dot{\gamma} = \sqrt{2\vec{\sigma} : \vec{\sigma}} \tag{15}$$

This analytical model predicts shear thinning for n < 1, and equations 16 and 17 are valid.

$$\sigma = \frac{F}{S} = \eta \frac{dv}{dy} \tag{16}$$

$$\sigma_{y_x} = \eta\dot{\gamma}_{y_x} \tag{17}$$

Relationship between shear stress τ and shear rate γ is usually plotted in log - log coordinates, whereas for a shear-thinning fluid it can be approximated by a straight line over an interval of shear rate (equation 18). Then the viscosity can be expressed as in equation 19 and power law fluid is given in equation 20.

$$\sigma = m(\dot{\gamma})^n \tag{18}$$

$$\eta = m(\gamma)^{n-1} \tag{19}$$

$$\nu = \eta\rho^{-1} \Rightarrow \eta = \nu \cdot \rho \tag{20}$$

The velocity can be expressed as in equations 21, 22. In shear-thinning fluids, equations 23, 24 are valid.

$$\nu \cdot \rho = m(\dot{\gamma})^{n-1} \tag{21}$$

$$\nu = \frac{m(\dot{\gamma})^{n-1}}{\rho} \tag{22}$$

$$\lim_{y_{yx}\to o} \frac{\sigma_{yx}}{\dot{\gamma}_{yx}} = \eta_0 \tag{23}$$

$$\lim_{y_{yx}\to \infty} \frac{\sigma_{yx}}{\dot{\gamma}_{yx}} = \eta_\infty \tag{24}$$

In most cases, the value of η_∞ is only slightly higher than the solvent viscosity η_0. Parameter m is the consistency index (viscosity factor) with units [Pas^n], where n is flow index (shear thinning factor), with values of 0 < n < 1. In non-Newtonian fluids, one cannot talk about viscosity, since the relationship between the applied shear stress and the shear rate is not constant. The viscosity function is called apparent viscosity, and is a function of the shear rate, as given in equation 25.

$$\eta = \frac{\sigma}{\gamma} = \eta(\gamma) \neq cons\tan t \tag{25}$$

When a liquid flows through a tube it forms a velocity gradient, and a shearing effect occurs. Some methods have been developed to measure the flow properties of fluids by using capillary tubes through which a fluid is forced to flow due to applied pressure or hydrostatic pressure. If the volumetric flow, tube dimensions and applied pressure are known, curves of flow can be plotted and the apparent values of the viscosity can be calculated. Certain assumptions should be made to develop general equations that allow calculation of the shear rates and shear stresses for a specific point in the tube.

Equations 26 – 28 are valid for both non-Newtonian and Newtonian fluids, where q is the volumetric flow through the capillary of length l and radius R, and P is the applied pressure. In these equations, the value of b can be calculated by plotting ($4q/R^3$) vs. ($\Delta PR/2$ l) in double logarithmic coordinates, where b represents the slope of the straight line formed in such a way.

$$\gamma = \frac{3+b}{4\left(\frac{4q}{\pi R^3}\right)} \tag{26}$$

$$b = \frac{d\log\left(\frac{4q}{\pi R^3}\right)}{d\log\left(\frac{\Delta pR}{2l}\right)} \tag{27}$$

$$\gamma = \frac{4q}{R^3} \tag{28}$$

Fluid friction factor for laminar flow can be expressed as in equation 29, where R_{eG} is generalized Reynolds number (equation 30), where d – diameter; v – mean velocity of the fluid; ρ – density of the fluid; n – shear thinning factor; m – viscosity factor.

$$f = \frac{16}{R_{e_G}} \tag{29}$$

$$R_{e_G} = \frac{d^n \cdot v^{2-n} \cdot \rho}{8^{n-1} \cdot m} \cdot \left(\frac{4n}{1+3n}\right)^n \tag{30}$$

4. MATERIALS AND METHODS

We used gelatin-based hydrogel for 3D bioprinting. We added 15 g of food grade gelatin

to 100 ml of water to achieve the concentration of 13.04 wt% and the mixture stayed at room temperature for 5 minutes. Afterwards it was heated to 50 °C and the liquefied solution was loaded in the syringe. The sample was printed by using extrusion-based bioprinter (Tissue Scribe, 3D Cultures) with 10 ml syringe and 0.838 mm diameter needle.

We used open-source slicer software Cura to set the printing parameters, as given in Table 1. Printing speed (nozzle speed while extruding) was 0.1 mm/s, printing platform was at room temperature while the material-loaded syringe was heated to 43 °C. After several trials, this was found to be the most suitable temperature for this hydrogel. At lower temperatures the needle got clogged while at higher temperatures the viscosity was too low and no shape of the printed structures could be retained.

Table 1. 3D printing parameters for gelatin-based hydrogel.

Layer Height	1 mm
Wall Thickness (Shell)	2 mm
Infill	33%
Printing Temperature	43 °C
Platform Temperature	Room Temperature
Print speed	0.1 mm/s
Travel speed	250 mm/s

We calculated parameter optimisation index (POI) for this hydrogel, with our experimental data from 3D bioprinting. Plunger diameter was 14.2 mm, plunger speed was 0.011 mm/s and inner diameter of 18G needle is 0.838 mm. With these values we can calculate velocity v_2, and pressure, where hydrogel solution density was taken as 0.989 kg/dm^3, height was 9.3 cm, line width was 3 mm and needle gauge was 18G. We calculated Reynolds number for our gelatin sample using equation (28) and friction factor using equation (29).

5. RESULTS AND DISCUSION

Bioprinting of gelatin mixed only with water is possible, but dimensional accuracy is lacking, as shown in Table 2. After several variations of 3d printing parameters, we determined those values that allowed printing, but the quality of samples was not satisfying for further manipulation of samples. However, it allowed us to validate analytical model of shear thinning presented in previous chapter. This model, along with optimisation method, can further enable more precise determination of printing parameters for the best quality design of scaffold 3d geometry and structure, with other gelatin-based hydrogels.

Table 2. Change in cross-sectional dimensions of the 3D printed sample of gelatin-based scaffold.

	CAD model	Immediately after printing	After 4 days	After 7 days
Sample length [mm]	30	34	27.4	27
Sample width [mm]	20	23	17.6	17.5
Sample height [mm]	4	10	5.4	4.5

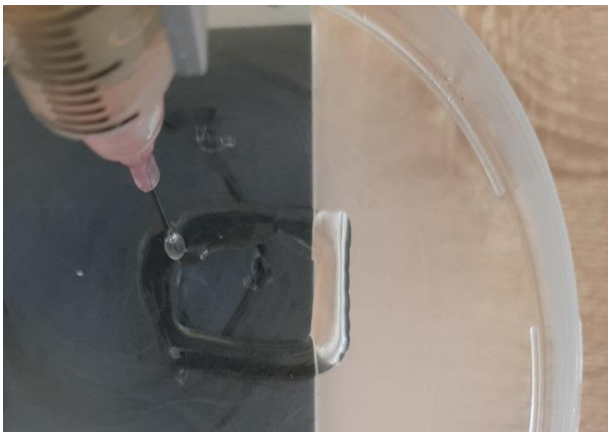

Fig. 2. A droplet visibly emerging from the syringe.

This low dimensional accuracy can be elaborated mainly due to formation of droplets, instead of thin filament at the outlet of the needle, as shown in Fig. 2. It can be seen that droplet size is noticeably larger than the needle diameter thus indicating high surface tension. Accordingly, the line width was significantly wider than the needle diameter (nozzle opening size). Increase in line width due to line collapsing is noticed even in successful prints, where filament formation is facilitated [17].

3D CAD model used to generate G-code for this sample had its rectangular cross-section dimensions assigned to be 30 x 20 x 4 mm. The

sample was measured several times. Immediately after the printing its dimensions were 34 x 23 x 10 mm, with significant changes in comparison to design, especially related to sample height. The sample was stored in closed container in refrigerator and measured again after 4 and 7 days when it exhibited significant shrinkage, as shown in Table 2. It is obvious that water was evaporating rapidly. The sample had very small number of bubbles after the printing, and with time, number of bubbles increased, thus indicating certain chemical reactions. Gelatin-based hydrogels are organic in nature, meaning that it is prone to bacteria and mold growing. Some samples that were left at room temperature (around 27 °C during the day and around 20 °C during the night) exhibited significant bacteria and mold growing after only one day and were further unusable. Samples that were left in refrigerator did not show any signs of molding, even after 14 days. However, samples changed their dimensions over time, especially the sample height was decreased, and number of bubbles increased, as can be noticed in Fig. 3. Increase of bubbles was rapid in first 4 days, after which it significantly slowed.

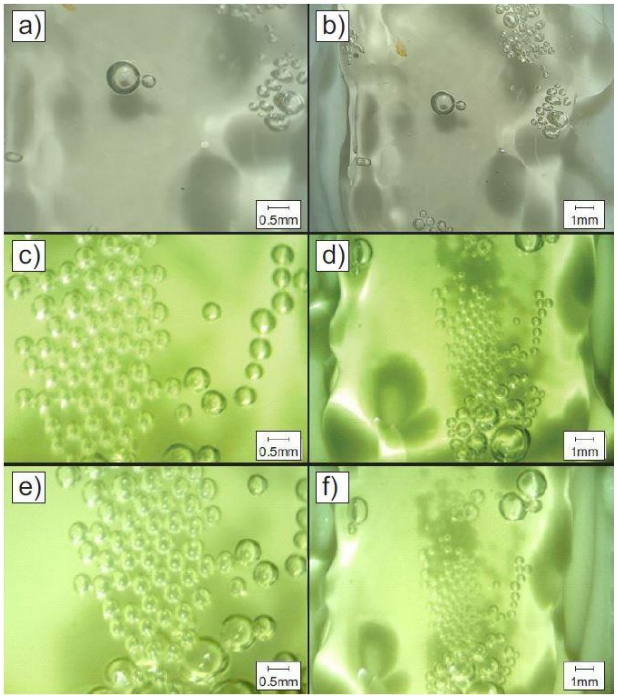

Fig. 3. Top view of the bioprinted gelatin sample over time: a), b) Right after printing; c), d) After 4 days; e), f) After 7 days

Droplet formation was fast enough for a printed line to appear as continuous, but as the layers went, geometry became increasingly distorted. We deposited 4 layers and the 4th one was very close to the needle tip, due to significant increase of real layer height in comparison to designed one. Geometry of the printed sample was visibly distorted due to droplet formation during the extrusion. Droplets of the first layer would fall and stick approximately where they were supposed to (according to the G-code) but in the next layers, the droplets were prone to slide over uneven surface of the previous layer and subsequently solidify in the incorrect position, thus significantly distorting the geometry. This gelatin hydrogel solution also showed very poor adhesion of subsequent layers. Also, sharp angles were very prone to errors in printing. When assessing the hydrogel printability there are many influential factors that need to be considered, such as printing distance, sharp angles, line collapsing, layer adhesion and accumulation of height errors [17].

Printing distance decreased from 13 mm at the beginning to 3 mm by the end of the printing process, meaning that real layer height was significantly larger than the setup of 1 mm (value set in the slicer software). This is another consequence of the droplet formation. However, after 4 days, the sample height decreased from 10 mm to 5.4 mm and further to 4.5 mm after 7 days (Table 2). Other two dimensions did not change that much over time, thus indicating that not only the evaporation of water is the reason of such discrepancies in dimensions. Lack of shear-thinning properties or thixotropic behaviour of gelatin-based hydrogels was studied also by other authors [18].

Figure 4 shows the sample after 4 days and if compared to images in Fig. 3, it can be seen that shear creep and sliding of layers occurred over time, along with increase of number of bubbles. Gilsenan and Ross-Murphy [19], studied creep of gelatin gels and showed that there are co-dependencies between hydrogel concentrations, dynamic viscosity, and creep rheological behaviour. Shear creep of gelatin influences changes in dimensional measures of the sample over time and cannot be neglected, since it was evident very quickly, as shown in Figs. 3 and 4. It can be seen that upper layers slid over lower ones, and base layer spread out under the weight of upper layers. This clearly indicated that pure gelatin hydrogel did not provide necessary mechanical properties to support further cell seeding.

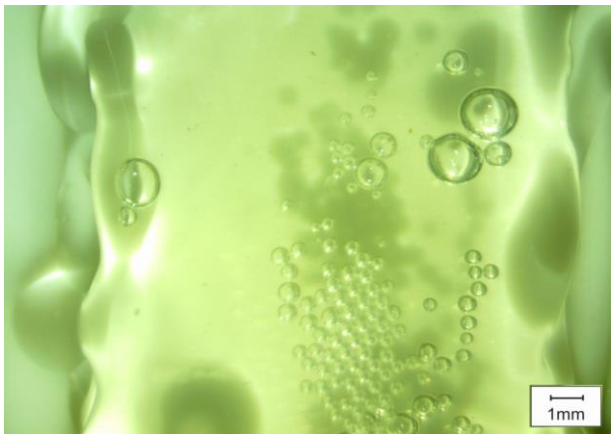

Fig. 4. Sample after 4 days, showing sliding, shear creep and increased number of bubbles in top surface layer.

The value of calculated POI from equation (4), was 0.02 1/mmPa. Further experiments would be needed for normalisation of this value relative to the maximum value in the series of printing samples with different material and process parameters.

The consistency index (viscosity factor), m, and flow index (shear thinning factor), n, of gelatin can be found in literature [20], and we adopted the following values: m = 7 Pas^n, n = 0.989. Accordingly, we calculated Reynolds and friction factor as follows.

$$R_{eG} = 0.5962 \cdot 10^{-7} \tag{31}$$

$$f = 0.268 \cdot 10^{-5} \tag{32}$$

It can be seen that values of Reynolds number and friction factor both correspond to those that can be found in the literature. The value of friction factor is very small which is favorable for easy sliding of layers over each other, what is in consistence with Figs. 3 and 4, that indicated layer sliding. Additionally, solidification of gelatin hydrogel occurred very fast after the printing and prevented good layer adhesion.

After 14 days, the sample was very thin, without mechanical strength and also showed initial signs of cracks, as shown in Fig 5. Network of very thin cracks can be seen throughout the whole sample and were especially exhibited in zones where bubbles initially appeared and were still visible after 14 days (Fig 5).

Our results showed that gelatin hydrogel that is made only by mixing gelatin with water is prone to significant changes in short time.

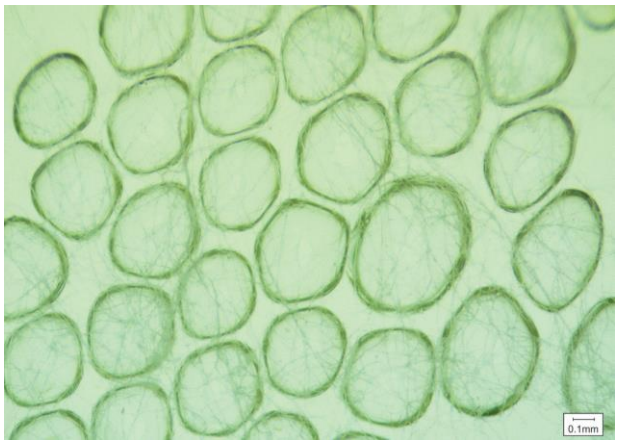

Fig. 5. Sample after 14 days, showing initial signs of cracks.

Cell seeding on bioprinted scaffolds needs appropriate timeframe during which the scaffold geometry and structure should not drastically change. We demonstrated that analytical model of shear thinning and friction factor can be used to assist in determination of the most optimal material and process parameters. Further tests with gelatin-based hydrogel with additional compounds (such as methyl methacrylate, MMA, or hydroxyapatite, HAp) are foreseen, together with optimisation of 3D bioprinting parameters to achieve the optimal bioscaffold.

6. CONCLUSIONS

Our results showed that behaviour of hydrogel solutions during 3D bioprinting is highly dependent on numerous influential parameters. Material properties such as chemical constituents and gel concentration are the most influential factor, but preparation procedure also has the essential influence on printability of hydrogel. Shear thinning property of the hydrogel determines the possibility to form thin filament instead of the droplet on the output of the needle, during the extrusion-based printing, thus significantly influencing dimensional accuracy of the printed scaffold. Proposed analytical shear thinning model supported experimental data and showed that it can be used to assist in optimisation of material and process parameters of 3D bioprinting. Very low friction factor of the hydrogel solution flow is necessary, but it should be optimised in such way to prevent sliding of layers over each other during the printing, in order to provide layer adhesion. Shear creep was noticed, along with exhibited sliding of layers over time, after the

printing. Further research is needed related to material constituents of the hydrogel, as well as printing parameters, aiming at optimal 3D bioprinting of bioscaffolds.

Acknowledgement

This research was supported by 3DP-ELN and BIOLAB projects, Ministry of Education, Science and Technological Development, Republic of Serbia.

REFERENCES

[1] I. Nakic, D. Istokovic, M. Perinic, G. Cukor, *Implementation of additive technology in medicine*, Mechanical Technology and Structural Materials, vol. 2017, iss. 1, pp. 89-98, 2017.

[2] D. Singh, D. Thomas, *Advances in medical polymer technology towards the panacea of complex 3D tissue and organ manufacture*, American Journal of Surgery, vol. 217, iss. 4, pp. 807-808, 2019, doi: 10.1016/j.amjsurg.2018.05.012

[3] S. Rhee, J.L. Puetzer, B.N. Mason, C.A. Reinhart-King, L.J. Bonassar, *3D Bioprinting of Spatially Heterogeneous Collagen Constructs for Cartilage Tissue Engineering*, ACS Biomaterials Science and Engineering, vol. 2, iss. 10, pp. 1800-1805, 2016, doi: 10.1021/acsbiomaterials.6b00288

[4] M.M. Laronda, A.L. Rutz, S. Xiao, K.A. Whelan, F.E. Duncan, E.W. Roth, T.K. Woodruff, R.N. Shah, *A bioprosthetic ovary created using 3D printed microporous scaffolds restores ovarian function in sterilized mice*, Nature Communications, vol. 8, no. 15261, 2017, doi: 10.1038/ncomms15261

[5] K. Markstedt, A. Mantas, I. Tournier, H. Martínez Ávila, D. Hägg, P. Gatenholm, *3D Bioprinting Human Chondrocytes with Nanocellulose–Alginate Bioink for Cartilage Tissue Engineering Applications*, Biomacromolecules, vol. 16, iss. 5, pp. 1489-1496, 2015, doi: 0.1021/acs.biomac.5b00188

[6] D. Nguyen, D.A. Hägg, A. Forsman, J. Ekholm, P. Nimkingratana, C. Brantsing, T. Kalogeropoulos, S. Zaunz, S. Concaro, M. Brittberg, A. Lindahl, P. Gatenholm, A. Enejder, S. Simonsson, *Cartilage Tissue Engineering by the 3D Bioprinting of iPS Cells in a Nanocellulose/Alginate Bioink*, Scientific Reports, vol. 7, no. 658, 2017, doi: 10.1038/s41598-017-00690-y

[7] Z. Tan, C. Parisi, L. Di Silvio, D. Dini, A.E. Forte, *Cryogenic 3D Printing of Super Soft Hydrogels*, Scientific Reports, vol. 7, no. 16293, 2017, doi: 10.1038/s41598-017-16668-9

[8] S.A. Irvine, A. Agrawal, B.H. Lee, H.Y. Chua, K.Y. Low, B.C. Lau, M. Machluf, S. Venkatraman, *Printing cell-laden gelatin constructs by free-form fabrication and enzymatic protein crosslinking*, Biomedical Microdevices, vol. 17, no. 16, 2015, doi: 10.1007/s10544-014-9915-8

[9] C.-C. Kuo, H. Qin, Y. Cheng, X. Jiang, X. Shi, *An integrated manufacturing strategy to fabricate delivery system using gelatin/alginate hybrid hydrogels: 3D printing and freeze-drying*, Food Hydrocolloids, 2021, doi: 10.1016/j.foodhyd.2020.106262

[10] A. Shafiee, E. Ghadiri, H. Ramesh, C. Kengla, J. Kassis, P. Clavert, D. Williams, A. Khademhosseini, R. Narayan, G. Forgacs, A. Atala, *Physics of bioprinting*, Applied Physics Reviews, vol. 6, iss. 2, 2019, doi: 10.1063/1.5087206

[11] F.L.C. Morgan, L. Moroni, M.B. Baker, *Dynamic Bioinks to Advance Bioprinting*, Advanced Healthcare Materials, vol. 9, iss. 15, 2020, doi: 10.1002/adhm.201901798

[12] N. Busarac, *Influential parameters of 3D bioprinting quality*, Bachelor thesis, Faculty of Engineering, University of Kragujevac, Kragujevac, 2020. (in Serbian)

[13] B. Webb, B.J. Doyle, *Parameter optimization for 3D bioprinting of hydrogels*, Bioprinting, vol. 8, pp. 8-12, 2017, doi: 10.1016/j.bprint.2017.09.001

[14] M. Trofa, G. D`Avino, *Sedimentation of Fractal Aggregates in Shear-Thinning Fluids*, Applied Sciences, vol. 10, iss. 9, pp. 1-20, 2020, doi: 10.3390/app10093267

[15] A. Ibarz, G.V. Barbosa-Canovas, *Unit Operation in Food Engineering*, Florida: Boca Raton, 2002.

[16] A. Khamoushi, A. Keramat, A. Majd, *One-Dimensional Simulation of Transient Flows in Non-Newtonian Fluids*, Journal of Pipeline Systems Engineering and Practice, vol. 11, iss. 3, pp. 1-16, 2020, doi: 10.1061/(ASCE)PS.1949-1204.0000454

[17] Y. He, F. Yang, H. Zhao, Q. Gao, B. Xia, J. Fu, *Research on the printability of hydrogels in 3D bioprinting*, Scientific Reports, vol. 6, no. 29977, 2016, doi: 10.1038/srep29977

[18] L.J. Djakovic, V. Sovilj, S. Milosevic, *Rheological Behaviour of Thixotropic Starch and Gelatin Gels*, Starch, vol. 42, iss. 10, pp. 380-385, 1990, doi: 10.1002/star.19900421004

[19] P.M. Gilsenan, S.B. Ross-Murphy, *Shear creep of gelatin gels from mammalian and piscine collagens*, International Journal of Biological Macromolecules, vol. 29, iss. 1, pp. 53-61, 2001, doi: 10.1016/S0141-8130(01)00149-0

[20] J. Ahmed, *Rheological Properties of Gelatin and Advances in Measurement*, Advances in Food Rheology and Its Applications, Elsevier Inc., pp. 377-404, 2017.